Surface Science 604 (2010) 1476–1480

Contents lists available at ScienceDirect

Surface Science

journal homepage: www.elsevier.com/ locate/susc

Strontium oxide segregation at $SrLaAlO_4$ surfaces

A.E. Becerra-Toledo *, L.D. Marks

Northwestern University, Department of Materials Science and Engineering, Evanston, IL 60208, USA

ARTICLE INFO

Article history:
Received 18 August 2009
Accepted 10 May 2010
Available online 19 May 2010

Keywords:
Electron microscopy
Surface segregation
Diffusion and migration
SrLaAlO4
Single crystal surfaces

ABSTRACT

We report observable segregation of strontium oxide at the surface of strontium lanthanum aluminate single-crystals annealed in oxidizing conditions. Electron microscopy imaging and energy-dispersive X-ray spectroscopy showed that Sr and O segregation occurs on strontium lanthanum aluminate surfaces in the form of polycrystalline islands. The appearance of islands on the (100) and other high-free energy surfaces is strongly suggestive of rocksalt SrO formation. The loss of strontium oxide from the bulk is not compensated solely by point defects, but rather by non-stoichiometric stacking faults which locally result in stable perovskite structures.

1. Introduction

Strontium lanthanum aluminate, $SrLaAlO_4$, has become one of the favored substrate materials for epitaxial growth of high-T_c superconducting thin films for microwave and far-infrared applications [1–3]. It exhibits excellent lattice match with superconducting cuprates, remarkable dielectric, elastic and optical properties [3–7], as well as high chemical stability [8]. Its single-crystal bulk properties have been widely studied, as well as the effects of its crystal growth method and growth conditions [9–15]. However, there is a surprising lack of surface-specific literature on this material.

Studying surface stabilization phenomena in metal oxides is essential in order to fully understand these mechanisms at the nanoscale and to enhance the potential of metal oxides in applications such as thin film growth and heterogeneous catalysis. Strontium lanthanum aluminate crystallizes in the perovskite-like K_2NiF_4 structure ($a = b = 3.756$ Å, $c = 12.64$ Å [4]) with space group I4/mmm, as shown in Fig. 1a; this material offers an additional degree of complexity due to the shared occupancy of the nine-fold coordination site by Sr and La cations, which are distributed statistically. In this context, $SrLaAlO_4$ goes beyond simpler systems that have been studied to date, opening the door to new questions. Is the surface behavior similar to what goes on in relatively simple systems such as perovskite $SrTiO_3$ [16–18] or $LaAlO_3$ [19], or does the mixture of 2+ and 3+ cations allow different phenomena to occur at the surface? What role do bulk defects play in the stabilization of the surface if there is a change in stoichiometry, either as point or extended defects? The aim of this work is to examine the behavior of the $SrLaAlO_4$ (001) and (100) surfaces upon thermal treatment under oxidizing conditions. We find that this system is fundamentally different from other comparable oxides; it shows strong surface segregation of strontium oxide at high temperatures, in the form of islands, as demonstrated by transmission electron microscopy (TEM), scanning electron microscopy (SEM) and energy-dispersive X-ray spectroscopy (EDS).

2. Experimental methods

Single-crystal $SrLaAlO_4$ (001)- and (100)-oriented wafers ($10 \times 10 \times 0.5$ mm^3, 99.99% purity, grown by the Czochralski method, one side EPI polished) were purchased from a commercial vendor, MTI Corporation. Inductively coupled plasma atomic emission spectroscopy (ICP-AES) measurements were performed on some of the material with a Varian Vista-MPX instrument for stoichiometry verification. The (001) wafers were cut into 3 mm-diameter disks using an ultrasonic disk cutter. Each disk was subsequently mechanically thinned with SiC polishing paper to a thickness of ~100 μm, dimpled, and finally ion milled to electron transparency using 3.8–4.5 kV Ar^+ ion beams in a Gatan Precision Ion Polishing System (PIPS). Samples were annealed in a tube furnace in a flow of O_2 gas in two steps: first, a preliminary anneal for 3 h at 650–700 °C, in order to revert most of the damage induced during preparation and to recover the original stoichiometry; and second, a longer 6-hour anneal at a chosen high temperature in the range of 900–1300 °C, which was the main variable. There was no active external cooling afterwards, but the cooling rate was capped at −10 °C/min. Transmission electron microscopy and diffraction experiments were carried out on a JEOL JEM-2100F microscope, operated at 200 kV and equipped with an Oxford Instruments INCAx-stream EDS detector. EDS microanalysis was performed in scanning transmission (STEM) mode, while high-

* Corresponding author. Tel.: +1 847 491 7809; fax: +1 847 481 7820.
E-mail address: andres@u.northwestern.edu (A.E. Becerra-Toledo).

0039-6028/$ – see front matter © 2010 Elsevier B.V. All rights reserved.
doi:10.1016/j.susc.2010.05.011

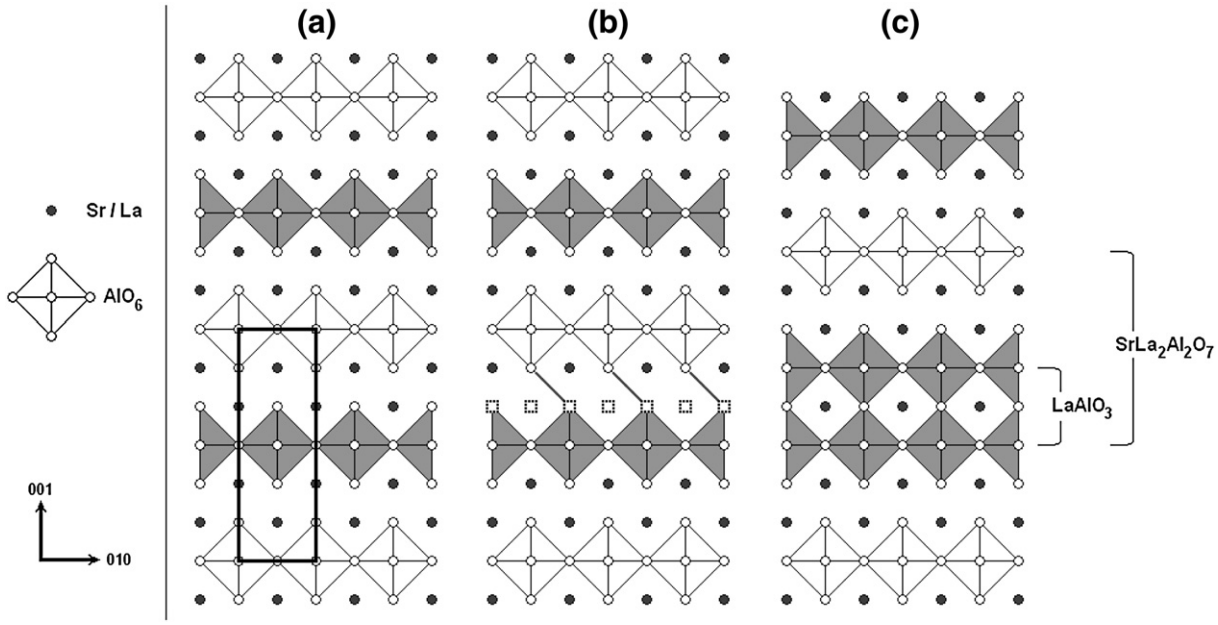

Fig. 1. (a) [100] projection of bulk $SrLaAlO_4$, unit cell outlined. (b) Removal of a layer of SrO and diagonal lines indicating subsequent <1/2 1/2 *z*> crystallographic shear. (c) Resulting structure with stacking fault. All octahedra are Al-centered; gray coloring indicates an out-of-page half-unit-cell shift with respect to white octahedra. O atoms are white circles and Sr/La atoms are dark circles. Empty squares denote vacant sites.

resolution imaging was done under conventional parallel-beam illumination. Measurement of lattice features was calibrated to the known bulk spacings in $SrLaAlO_4$.

The strong (001) cleavage in $SrLaAlO_4$ [3,4] made it unviable to thin the (100)-oriented samples to electron transparency. Therefore, (100) and (001) bulk crystals were annealed as received at the same high temperature and same environment for subsequent SEM-EDS analysis with a Hitachi S-3400N-II microscope, operated at 5 kV and outfitted with an Oxford Instruments INCAx-act EDS detector. SEM imaging was performed in secondary-electron detection mode for topographical information.

3. Results

As determined via electron diffraction, there was no evidence of surface ordering with non-bulk periodicity at any of the annealing conditions explored during these experiments. Temperatures below 1200 °C did not yield any apparent morphological changes. However, annealing at 1250–1300 °C for 6 h in oxidizing conditions resulted in the microstructure shown in Fig. 2 in a (001)-oriented sample. In thin regions of the sample, numerous holes formed, but the specimen remained a single crystal, as indicated by the diffraction patterns. Distinct faceting, mostly along {100} and {110}-type surfaces, is clearly observable. This microstructure is similar to what has been seen in previous studies of metal oxides [16–19].

STEM-EDS line scans were performed on (001)-oriented samples, scanning from the bulk towards the edges. A semi-quantitative analysis followed, which showed a marked increase in Sr content, relative to La and Al, near some {100} and {110} surfaces; this was highly suggestive of strontium oxide surface segregation. High-resolution TEM images validated the hypothesis of SrO presence at these surfaces. For example, Fig. 3 reveals periodic lattice features which match – within a few percent error – a {110}-type rocksalt SrO orientation on a {100} $SrLaAlO_4$ surface; there is some slight distortion in the SrO lattice in order to accommodate for the lattice mismatch of ~3%. The surfaces perpendicular to <001> are not, however, uniformly covered in a few monolayers of this Sr-rich material; many segments remain clean of it.

Aside from the segregation of a few monolayers of strontium oxide on some surfaces, there were also some regions where relatively large amounts of SrO formed as a separate phase. This occurred both in the form of precipitates within the $SrLaAlO_4$ matrix as well as exposed

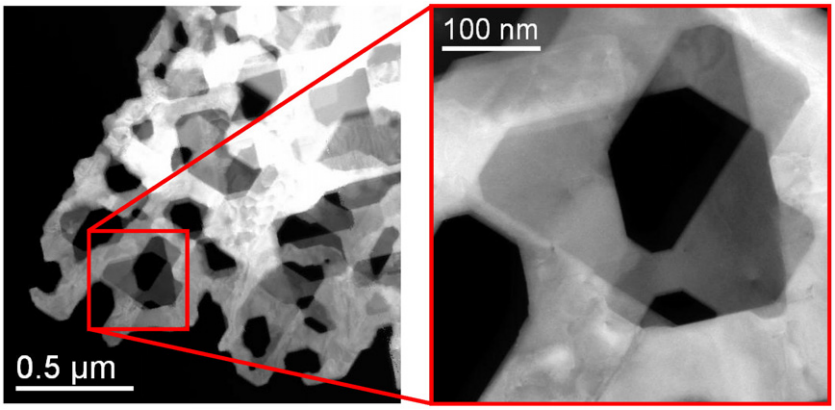

Fig. 2. [001]-zone high-angle annular dark field scanning electron micrograph of $SrLaAlO_4$ crystal, after annealing at 1300 °C in O_2.

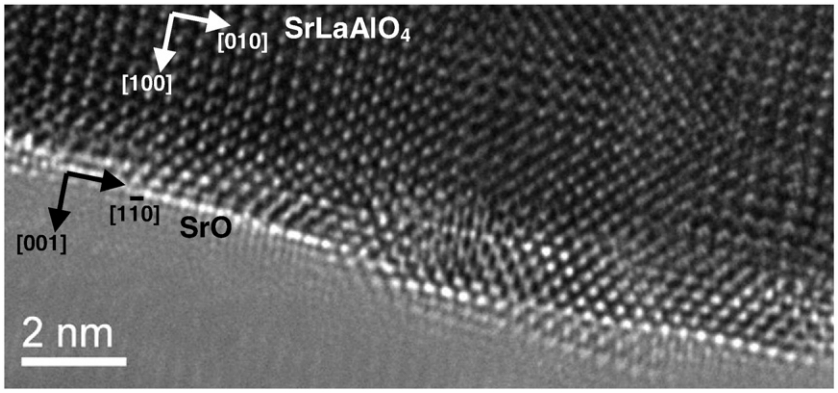

Fig. 3. High-resolution electron micrograph, showing formation of layers of SrO on a $SrLaAlO_4$ (100) surface.

areas (as shown in Fig. 4). EDS elemental mapping confirmed that these secondary phases consist predominantly of strontium and oxygen. The weak Al and La signals from said areas imply that these elements were present, but merely in solid solution within the SrO matrix. High-resolution TEM imaging of these secondary phases support this finding: lattice spacings matching the {110}, {111} and {210} rocksalt SrO interplanar distances were visible within these phases, which were not single-crystalline.

Thermal treatment of (100)-oriented as-received samples under the same annealing conditions confirmed the segregation of SrO at this surface. SEM imaging revealed the presence of surface islands on the annealed samples which had a random positional distribution as well as a broad range of sizes, the largest observed island being roughly 50 μm wide. The (001)-oriented as-received samples showed a similar behavior upon annealing, except that the surface islands were as large as 500 μm wide and very few small features were observed. Fig. 5 shows a large island on this surface, which shows obvious signs of agglomeration of multiple particles. The estimated island coverage was 4% on the (100) surface and 2.5% on the (001) surface, with a 1% margin of error.

SEM-EDS elemental mapping was carried out on the islands with the electron beam perpendicular to the surface and set to a relatively low voltage of 5 kV. This minimized the effects of sample charging and enhanced the surface sensitivity of the technique. The results were qualitatively the same for both surface orientations. A typical set of elemental maps is also presented in Fig. 5. These results verify that the aforementioned features correspond to the formation of SrO-rich islands on low-index $SrLaAlO_4$ surfaces.

It is also possible to address the mechanism by which the $SrLaAlO_4$ bulk remains stable in spite of the preferential migration of Sr and O to the surface and the consequent non-stoichiometry. Said bulk stabilization is linked to the appearance, in (001)-oriented TEM samples, of a large number of planar defects (Fig. 6a) after the high temperature anneal; no such features were observed with lower temperatures. These defects exhibit jagged boundaries, always along [100] and [010] directions. Upon closer examination in high-resolution mode, we find that the lattice contrast in these planar defects exhibits half-unit-cell shifts with respect to the rest of the crystal (Fig. 6b). Therefore, these features are explained as disordered stacking faults; the observed shifts correspond to a $<1/2\ 1/2\ z>$ crystallographic shear ($z \sim 1/6$), as can be seen schematically in Fig. 1b; the loss of a SrO (001) layer in $SrLaAlO_4$ favors said effect. Similar crystallographic shear mechanisms has been observed in perovskite systems [20–22], as well as the broader Ruddlesden-Popper family [23], although they have rarely been discussed in combination with surface segregation and never before have both phenomena been coupled through direct observation.

4. Discussion

This system does not form a periodic surface reconstruction such as those observed under similar conditions in $SrTiO_3$ and $LaAlO_3$ [16–19]. Instead, the surfaces are stabilized via SrO segregation. To the best of our knowledge, no such segregation behavior has been observed in materials with the perovskite-like K_2NiF_4 structure. We believe that this phenomenon is enabled by two main factors: the easy

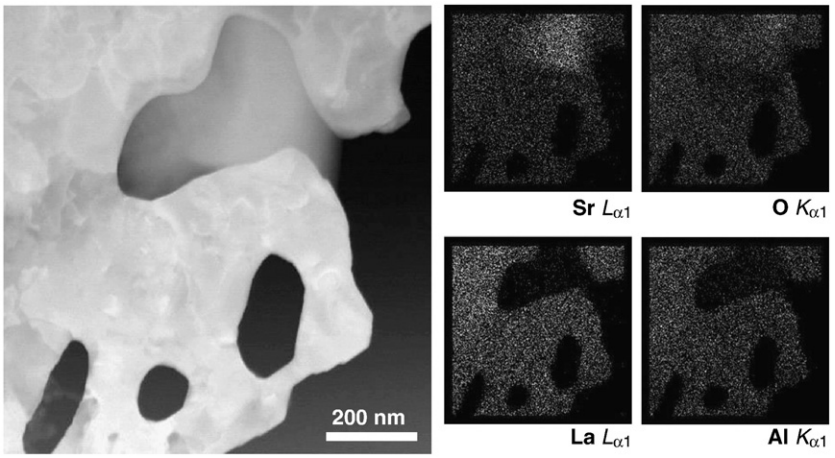

Fig. 4. (Left) Dark-field STEM image with [001] zone axis. (Right) EDS elemental maps, showing the presence of a Sr-rich secondary phase.

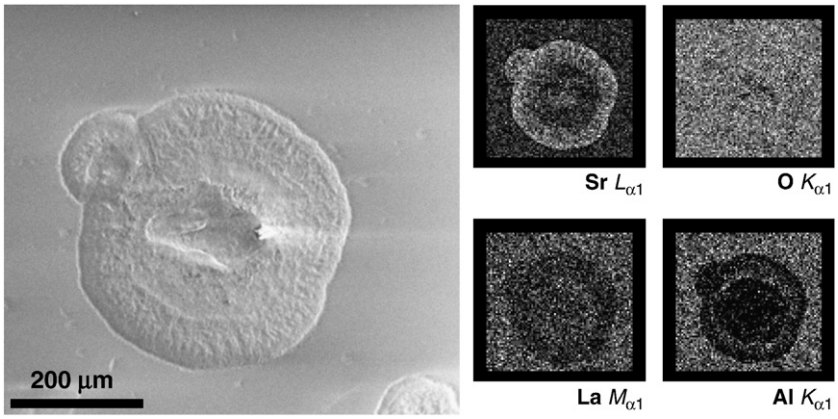

Fig. 5. (Left) Plan-view scanning electron image of feature on a $SrLaAlO_4$ (100) surface. (Right) EDS elemental maps corresponding to the same feature.

compensation for the bulk non-stoichiometry via an accessible stacking-fault mechanism and the configurational entropy contribution by the bulk defects.

As described above, the $SrLaAlO_4$ bulk accommodates for the Sr and O deficiency by generating stacking faults. The crystallographic shear results in the alternation of AlO_2–LaO–AlO_2 layers in a configuration of corner-sharing octahedra along the <001> direction. In short, this generates thin regions consisting of perovskite $LaAlO_3$, which is highly stable. Moreover, the *a* lattice parameter of $SrLaAlO_4$ (3.756 Å) has a very small (<1%) mismatch with the pseudocubic $LaAlO_3$ lattice parameter (3.790 Å) [24]. This process is equivalent to the subtraction of a Ruddlesden-Popper (RP) fault, for it locally converts a RP phase ($AO\cdot(ABO_3)_n$; A = Sr/La, B = Al, $n = 1$) [25,26] into a perovskite phase, not vice versa. We therefore call these defects *inverse* RP faults.

Upon broader inspection, the resulting structure may also be attributed to a region of $SrLa_2Al_2O_7$, instead of $LaAlO_3$, as illustrated in Fig. 1c. In fact, the $LaAlO_3$–$SrLaAlO_4$ phase diagram [27] shows only $SrLa_2Al_2O_7$ as a secondary phase in nearly pure $SrLaAlO_4$ for temperatures above 1300 °C, which is coincidentally our upper limit. It is plausible that a longer or higher-temperature anneal would result in the ordering of the inverse RP faults matching the periodicity of said phase.

One possible explanation for the observed surface segregation is that the samples are not stoichiometric. $SrLaAlO_4$ crystal growth from a stoichiometric melt results in crystals exhibiting cracks and undesired inclusions. Therefore, it is common to use some excess Sr precursor in the melt in order to obtain high-quality crystals [9]. This is typically explained as some Sr ions substituting for La (plus half an oxygen vacancy per cation substitution), which is easy to accommodate due to the nearly identical cationic radii [10]. Indeed, the commercial vendor from which the crystals were purchased acknowledges that 0.5% excess Sr (by weight) is regularly added to the starting mix for the growth of $SrLaAlO_4$ [28].

However, the ICP-AES measurements yield a Sr/La ratio of 0.999 ± 0.002, which indicates that the as-received crystals are stoichiometric, within the accuracy of the technique. Any Sr excess, if at all present, is negligible and cannot account for the observed level of surface segregation. Moreover, even in the case of higher Sr content, it is not clear that there would be a strong driving force for segregation other than the factors discussed above. In particular, the aforementioned size similarity between Sr^{2+} and La^{3+} implies that the resulting lattice strain would be small.

Another possible explanation is that segregation of SrO to the surface reduces the surface free energy. Unfortunately, without a definitive model of the surface structure it is hard to estimate the relevant energies; even if one was available, calculating the energetics of a disordered solid solution such as this is hard even in the bulk, let alone at a surface. It is also not clear why this should lead to several layers of SrO on the surface — except to relieve epitaxial strains, there is no clear reason why this should be preferred over a single layer. Hence this explanation appears to be a bit tenuous; while we cannot definitively rule it out, it is not completely consistent with the experimental data.

There is a simpler explanation. The configurational entropy (entropy of mixing) of these planar defects is large enough that at high temperatures the entropic component of the free energy can outweigh the defect formation enthalpy, including a potential increase in the surface energy. This can be inferred by a simple calculation, whereby the entropic component is calculated as $-T\Delta S = -k_B T \ln \Omega$, where Ω is the

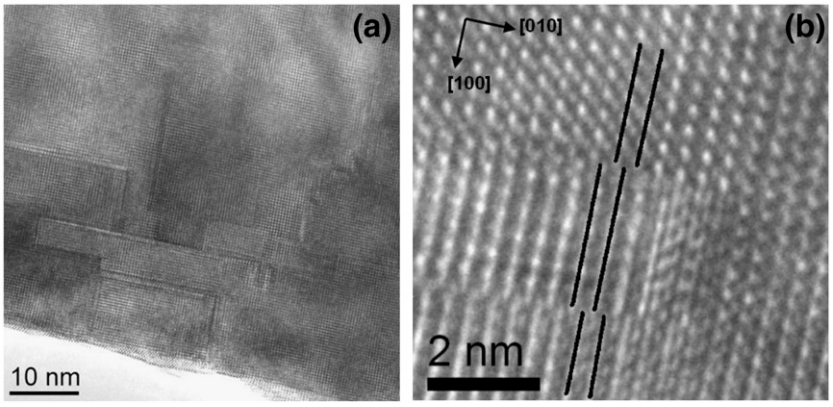

Fig. 6. (a) High resolution [001] image of planar defects in $SrLaAlO_4$ bulk. (b) Higher magnification of one such defect, with black lines denoting half-unit-cell shifts with respect to the bulk.

Table 1
Standard heat of dissociation into simpler oxides, calculated from thermodynamic data [34–36].

	ΔH^0 (eV)	ΔG^0 (eV)
$SrLaAlO_4 \rightarrow SrO + LaAlO_3$	0.28	0.29[a]
$SrLaAlO_4 \rightarrow SrO + ½\ La_2O_3 + ½\ Al_2O_3$	1.00	1.00
$SrTiO_3 \rightarrow SrO + TiO_2$	1.41	1.43

[a] Using $LaGaO_3$ standard entropy of formation from oxides as estimate for $LaAlO_3$.

number of possible configurations. In one dimension, this will depend on thickness, as there will be more possible stacking fault sites for a thicker specimen. For a single inverse RP fault in a $SrLaAlO_4$ sample only 100 nm thick (along the <001> direction), the entropic contribution to the free energy is approximately −0.69 eV at 1300 °C. We do not know the exact composition and structure of stable $SrLaAlO_4$ surfaces; it is thus impossible to precisely estimate the enthalpic cost of the stacking fault formation and the generation of a SrO–$SrLaAlO_4$ interface. However, as a reference for comparison, the dissociation enthalpy of $SrLaAlO_4$ into bulk SrO and bulk $LaAlO_3$ is calculated to be 0.28 eV per formula unit (Table 1). Most importantly, this explanation and only this one is consistent with the observation that the SrO surface islands are much larger in the thicker, as-received samples than in the thin regions examined using transmission electron microscopy.

For sufficiently large deviations from stoichiometry, it is reasonable that planar defects dominate over classical point defect explanations for bulk stabilization in $SrLaAlO_4$, as has been observed in other perovskite-like materials [20–23]. Nonetheless, the nucleation of these faults is presumably mediated by point defects, specifically vacancies. In a bulk structure of high packing density such as K_2NiF_4, one ought to expect Schottky-like disorder to dominate over Frenkel defects. Specifically, Sr–O vacancy pairs are perfect candidates for said fault nucleation, since they are easier to form and more mobile than larger complexes involving La or Al vacancies.

The surface segregation mechanism here is similar to, but fundamentally different from that proposed [29–31] to explain SrO surface segregation in $SrTiO_3$ under oxidizing conditions. In that hypothetical scheme, the dismantling of SrO layers would partially turn the original perovskite structure into regions with anatase-like stacking of TiO_2 units via <1/2 0 z>shears. As will be discussed elsewhere [32], this is inconsistent with the bulk phase diagram of SrO–TiO_2 where no surface phases are present. The question of whether $SrTiO_3$ samples where SrO segregation has been observed are from SrO-rich single crystals is worth further attention.

It should be noted that Sr-O vacancy pairs are also the lowest-energy point defect in strontium titanate [33], so the segregation of SrO at the surface – in both $SrTiO_3$ and $SrLaAlO_4$ – should be associated with driving up the number of bulk defects with extended high-temperature annealing. This explanation is more consistent with the larger literature where TiO_2-rich surfaces have been observed in $SrTiO_3$ upon annealing in oxidizing conditions; a plausible explanation is the reverse of what is found here, namely the formation of Ruddlesden-Popper faults in $SrTiO_3$ driven by entropic considerations, as will be discussed elsewhere [32]. A useful comparison is the standard heat of dissociation of $SrLaAlO_4$ and $SrTiO_3$ into simpler oxides; these values are shown, per formula unit, in Table 1. While all the surveyed reactions are endothermic, it is clear that the decomposition of strontium lanthanum aluminate into SrO and $LaAlO_3$ is easier than into all three binary oxides, and much easier than the decomposition of $SrTiO_3$ into its own constituent oxides.

5. Conclusions

Electron microscopy techniques and elemental microanalysis have been used in the present study to demonstrate that Sr and O segregate preferentially to $SrLaAlO_4$ surfaces upon thermal treatment under oxidizing conditions, forming strontium oxide islands whose characteristics depend on the surface exhibiting said segregation. This phenomenon is both allowed by the easy accommodation for SrO loss in the bulk as well as driven by the configurational entropy of the resulting defects.

The compensation mechanism in the bulk for the migration of strontium and oxygen consists predominantly of disordered inverse Ruddlesden-Popper faults. The dismantling of Sr-rich (001) layers results in crystallographic shear planes, which in turn generate plausibly stable structures such as $LaAlO_3$ or $SrLa_2Al_2O_7$. Surface segregation and bulk stacking faults have not been directly observed as a coupled system in the past, which opens up a new channel for stabilization that may occur in other material systems.

Acknowledgments

This work was supported by the US Department of Energy under grant number DOE DE-FG02-01ER45945. All TEM and SEM work was performed in the EPIC facility, part of the NUANCE Center at Northwestern University. The NUANCE Center is supported by NSF-NSEC, NSF-MRSEC, the Keck Foundation, the State of Illinois, and Northwestern University. A.E. Becerra-Toledo would also like to acknowledge Dr. Yingmin Wang's valuable instruction.

References

[1] X.Q. Liu, X.M. Chen, Y. Xiao, Mat. Sci. Eng., B 103 (2003) 276–280.
[2] R. Sobolewski, P. Gierlowski, W. Kula, S. Zarembinski, S.J. Lewandowski, M. Berkowski, A. Pajaczkowska, B.P. Gorshunov, D.B. Lyudmirski, O.I. Sirotinski, IEEE Trans. Magn. 27 (1991) 876–879.
[3] R. Brown, V. Pendrick, D. Kalokitis, B.H.T. Chai, Appl. Phys. Lett. 57 (1990) 1351–1353.
[4] R.D. Shannon, R.A. Oswald, J.B. Parise, B.H.T. Chai, P. Byszewski, A. Pajaczkowska, R. Sobolewski, J. Solid State Chem. 98 (1992) 90–98.
[5] M. Drozdowski, D. Kasprowicz, A. Pajaczkowska, J. Mol. Struct. 555 (2000) 119–129.
[6] J. Humlicek, R. Henn, M. Cardona, Phys. Rev. B 61 (2000) 14554–14563.
[7] G.X. Chen, Y.J. Ge, C.Z. Bi, X.G. Qiu, B.R. Zhao, J. Appl. Phys. 95 (2004) 3417–3421.
[8] I.A. Zvereva, L. Zueva, J. Choisnet, J. Mater. Sci. 30 (1995) 3598–3602.
[9] P. Byszewski, A. Pajaczkowska, J. Sass, K. Mazur, Cryst. Prop. Prep. 36–38 (1991) 560–564.
[10] A. Pajaczkowska, P. Byszewski, J. Cryst. Growth 128 (1993) 694–698.
[11] M. Berkowski, J. Fink-Finowicki, J. Sass, K. Mazur, Acta Phys. Pol. A 92 (1997) 201–204.
[12] J. Doerschel, I. Hähnert, R. Uecker, Acta Phys. Pol. A 92 (1997) 157–162.
[13] A. Pajaczkowska, A. Gloubokov, A. Klos, C.F. Woensdregt, J. Cryst. Growth 171 (1997) 387–391.
[14] W. Ryba-Romanowski, S. Golab, P. Deren, G. Dominiak-Dzik, W.A. Pisarski, Acta Phys. Pol. A 92 (1997) 191–196.
[15] D. Kasprowicz, M. Drozdowski, A. Pajaczkowska, Cryst. Res. Technol. 26 (2001) 1123–1126.
[16] N. Erdman, K.R. Poeppelmeier, M. Asta, O. Warschkow, D.R. Ellis, L.D. Marks, Nature 419 (2002) 55–58.
[17] N. Erdman, O. Warschkow, M. Asta, K.R. Poeppelmeier, D.R. Ellis, L.D. Marks, J. Am. Chem. Soc. 125 (2003) 10050–10056.
[18] C.H. Lanier, A. Van de Walle, N. Erdman, E. Landree, O. Warschkow, A. Kazimirov, K.R. Poeppelmeier, J. Zegenhagen, M. Asta, L.D. Marks, Phys. Rev. B 76 (2007) 045421.
[19] C.H. Lanier, J.M. Rondinelli, B. Deng, R. Kilaas, K.R. Poeppelmeier, L.D. Marks, Phys. Rev. Lett. 98 (2007) 086102.
[20] R.J.D. Tilley, J. Solid State Chem. 21 (1977) 293–301.
[21] A.A. Dobrikov, O.V. Presnyakova, V.I. Zaitsev, V.V. Prisedskii, G.F. Pan'ko, Krist. Tech. 15 (1980) 207–212.
[22] V.V. Prisedsky, V.P. Komarov, G.F. Pan'ko, V.V. Klimov, Ferroelectrics 23 (1980) 23–34.
[23] K. Hawkins, T.J. White, Philos. Trans. R. Soc. Lond. A 336 (1991) 541–569.
[24] S. Geller, V.B. Bala, Acta Crystallogr. 9 (1956) 1019–1025.
[25] S.N. Ruddlesden, P. Popper, Acta Crystallogr. 10 (1957) 538–539.
[26] S.N. Ruddlesden, P. Popper, Acta Crystallogr. 11 (1958) 54–55.
[27] V.F. Popova, E.A. Tugova, I.A. Zvereva, V.V. Gusarov, Glass Phys. Chem. 30 (2004) 564–567.
[28] MTI Corporation, personal communication.
[29] K. Szot, W. Speier, J. Herion, C. Freiburg, Appl. Phys. A 64 (1997) 55–59.
[30] K. Szot, W. Speier, Phys. Rev. B 60 (1999) 5909–5926.
[31] K. Szot, W. Speier, U. Breuer, R. Meyer, J. Szade, R. Waser, Surf. Sci. 460 (2000) 112–128.
[32] A.E. Becerra-Toledo, L.D. Marks, (in preparation).
[33] M.J. Akhtar, Z.U.N. Akhtar, R.A. Jackson, C.R.A. Catlow, J. Am. Chem. Soc. 78 (1995) 421–428.
[34] A.V. Novoselov, L.P. Ogodorova, G.V. Zimina, A. Pajaczkowska, Inorg. Mater. 36 (2000) 180–182.
[35] J. Cheng, A. Navrotsky, J. Mater. Res. 18 (2003) 2501–2508.
[36] CRC Handbook of Chemistry and Physics, CRC Press, 2007.